Acta Biomaterialia 7 (2011) 3555–3562

Contents lists available at ScienceDirect

Acta Biomaterialia

journal homepage: www.elsevier.com/locate/actabiomat

Comparison of the osteoblastic activity conferred on Si-doped hydroxyapatite scaffolds by different osteostatin coatings

Miguel Manzano [a,b,1], Daniel Lozano [c,1], Daniel Arcos [a,b], Sergio Portal-Núñez [c], Carlos Lopez la Orden [a,b], Pedro Esbrit [c,2], María Vallet-Regí [a,b,2,*]

[a] Departamento de Química Inorgánica y Bioinorgánica, Facultad de Farmacia, Universidad Complutense de Madrid, Madrid, Spain
[b] Centro de Investigación Biomédica en Red en Bioingeniería, Biomateriales y Nanomedicina, CIBER-BBN, Madrid, Spain
[c] Laboratorio de Metabolismo Mineral y Óseo, Instituto de Investigación Sanitaria-Fundación Jiménez Díaz, Madrid, Spain

ARTICLE INFO

Article history:
Received 15 March 2011
Received in revised form 3 June 2011
Accepted 5 June 2011
Available online 14 June 2011

Keywords:
Osteostatin
Osteoblastic function
Parathyroid hormone related protein
Silicon-doped hydroxyapatite scaffolds
Bioceramics functionalization

ABSTRACT

Parathyroid hormone-related protein (107-111) (osteostatin) induces osteogenic effects in osteoblasts in vitro and in regenerating bone in mice and rabbits. In this study we used osteoblastic MC3T3-E1 cell cultures to evaluate and compare the bioactivity of this peptide either adsorbed or covalently bound (by its C-terminus) to Si-doped hydroxyapatite (Si-HA) scaffolds after organic ($-NH_2$) functionalization. By these means osteostatin can be locally released or kept anchored to the scaffold surface. This was confirmed by chemical analysis and by testing the efficiency of osteostatin-loaded Si-HA scaffolds (placed in Transwell chambers) in healing a scratch wound in mouse pluripotent mesenchymal C3H10T1/2 cells. Our results show that exposure of MC3T3-E1 cell monolayers to Si-HA scaffolds with both types of osteostatin coating (deliverable or immobilized), in contrast to those without peptide, similarly stimulated cell growth and matrix mineralization. These findings demonstrate that osteostatin release from Si-HA scaffolds is not essential to promote osteoblastic growth and function in vitro, and lend credence to considering osteostatin a bone regenerating factor.

1. Introduction

Bone is a natural composite material mainly made of type 1 collagen and hydroxyapatite (HA). The former consists of a triple helix of protein chains that has high tensile and flexural strength and provides the bone tissue framework. The mineral content of bone, carbonate HA, is a crystalline calcium phosphate ceramic that provides the stiffness and high compressive strength of bone [1]. Bone can occur in two forms, trabecular and compact, and performs several functions in the body, such as a reservoir of calcium, providing a location for the haematopoietic marrow, and as a mechanical support for living tissues.

Bone injury can occur in a wide variety of clinical situations, and as a response bone regenerates and remodels itself [2]. Thus, when minor damage occurs bone tissue can repair itself by the activity of bone-forming cells (osteoblasts). However, when the defect exceeds a certain critical size, which might be produced by trauma or bone tissue necrosis and/or removal, bone healing is impaired. Traditionally graft implants and synthetic bone filler materials have been used to solve the latter problem. In this respect three-dimensional (3-D) scaffolds are recent osteoinductive devices which have proven efficacy in the so-called technology of regenerative biomedicine [3].

Bone tissue engineering requires that these 3-D scaffolds should be made in shapes to match that of the bone defect, mimicking trabecular bone in terms of porosity and chemical composition, and promoting bone growth. In addition, these scaffolds should exhibit the following features: (1) reabsorption at the same rate as new bone tissue is formed; (2) biocompatibility; (3) promotion of bone cell adhesion and bioactivity; (4) integration into the host bone minimizing the formation of scar tissue; (5) mechanical properties matching those of the host bone [4]. Thus an open macroporous structure with an average pore size ranging between 20 and 400 μm [5] is required for cell embedding, adherence and proliferation, leading to bone tissue in-growth and vascularization. Nowadays the fabrication of 3-D scaffolds exhibiting hierarchical pore networks can be easily done using computer controlled rapid prototyping, which also permits their shape adaptation to the specific requirements of bone tissue [6]. The materials employed to build this type of scaffold should thus have osteoinductive, osteoconductive and osteointegrating properties.

The development of biomaterials for tissue engineering applications has recently focused on the design of biomimetic materials

* Corresponding author at: Departamento de Química Inorgánica y Bioinorgánica, Facultad de Farmacia, Universidad Complutense de Madrid, Madrid, Spain. Tel.: +34 913941861.
E-mail address: vallet@farm.ucm.es (M. Vallet-Regí).
[1] These authors contributed equally to this manuscript.
[2] These authors have the same senior status with respect to this manuscript.

1742-7061/$ - see front matter © 2011 Acta Materialia Inc. Published by Elsevier Ltd. All rights reserved.
doi:10.1016/j.actbio.2011.06.004

capable of interacting with the surrounding tissues by biomolecular recognition. If bone is targeted, synthetic HA, $Ca_{10}(PO_4)_6(OH)_2$, is an optimal material in this regard, due to its chemical composition, which is similar to that of mineral apatite in this tissue. The biocompatibility of this material is excellent, but its bioactive behavior can be further improved by the introduction of Si into its structure [7]. Additionally, HA can be "decorated" with biopeptides, such as bone morphogenetic proteins, which are able to interact with the surrounding bone tissue. In this context we recently tested the osteogenic properties of a silica-based ordered mesoporous material coated with osteostatin, a pentapeptide (TRSAW, Thr-Arg-Ser-Ala-Trp) within the C-terminal sequence of parathyroid hormone related protein (PTHrP) [8]. This coating was found to be responsible for the ability of this type of material to induce both cell growth and the expression of several osteoblast differentiation factors in a well-characterized osteoblastic cell line. Taking into consideration that in vitro studies only provide a limited estimation of biomaterials activity, further in vivo studies with the aforementioned bioceramics were performed. This is an essential step in understanding the biocompatibility of a material and the frequently discussed issue of in vitro–in vivo correlation [9]. Thus the same silica-based bioceramics pre-tested in vitro were implanted in a cavitary defect in the epiphysis of the rabbit femur [10]. Histological examination revealed the absence of significant inflammation or bone resorption within the time of study (up to 8 weeks after implantation); on the other hand, new bone formation around the implant was demonstrated using immunohistochemistry and micro-computerized tomography (μCT) analysis.

In the present study we have confirmed and extended the osteoinductive properties of osteostatin by coating it onto synthetic Si-doped HA as a scaffold. We compared these properties when osteostatin was adsorbed or covalently bound by its C-terminus (Trp) to the surface of these scaffolds after organic functionalization. Retention of osteostatin in the latter scaffolds might represent an advantage in comparison with the former biomaterials, which would be prone to release the peptide into the surrounding medium in an in vivo setting, thus losing their bioactivity.

2. Materials and methods

2.1. Synthesis of Si-HA powder

Si-HA with the nominal formula $Ca_{10}(PO_4)_{5.7}(SiO_4)_{0.3}(OH)_{1.7}\square_{0.3}$, where □ indicates vacancies at the hydroxyl position, was prepared by aqueous precipitation reaction of $Ca(NO_3)_2{\cdot}4H_2O$, $(NH_4)_2HPO_4$ and $Si(CH_3CH_2O)_4$ solutions, as described elsewhere [11]. Briefly, a 1 M solution of $Ca(NO_3)_2{\cdot}4H_2O$ was added to solutions of $(NH_4)_2HPO_4$ and $Si(CH_3CH_2O)_4$ of stoichiometric concentration to obtain the composition described above. The mixture was stirred for 12 h at 80 °C. The pH was kept at 9.5 by NH_3 addition. During the reaction the pH was continuously adjusted to 9.5 to ensure constant conditions during synthesis. The precipitated Si-HA powder was treated at 700 °C to remove nitrates without introducing important changes in the structure and microstructure of the materials.

2.2. Preparation of Si-HA scaffolds with adsorbed osteostatin

3-D periodic macroporous scaffolds were prepared via direct write assembly of a Si-HA slurry, using 3-D printing rapid prototyping equipment (envisionTEC 3D Bioplotter™). The slurry was formed by slow addition under stirring of 29 g of Si-HA powder over a mixture of 23 ml of a monomeric aqueous solution composed of a mixture of 35 g methacrylamide and 5.75 g *N,N′*-methylene bisacrylamide as monomers in 250 ml, 60 μg ammonium persulphate as initiator and 3.0 g Darwan 811 as surfactant. The slurry obtained was housed in a syringe and deposited through a conical needle (diameter 580 μm) at the volumetric flow rate required to maintain a constant x–y table speed ($v = 3$ mm s^{-1}). The final dimensions of the scaffolds were 7 mm diameter and 5 mm high with interconnected pores (600 μm diameter). Once the scaffolds were prepared the polymers employed during the processing stage were thermally removed at 600 °C for 3 h. These non-functionalized scaffolds are denoted Si-HA(A) in the text below.

Si-HA(A) scaffolds were then loaded with synthetic PTHrP(107-111) (Bachem, Bubendorf, Switzerland) by soaking them in a solution of this peptide (100 nM) in 1 ml of phosphate-buffered saline (PBS) solution at 4 °C under stirring for 24 h. Release of this peptide from the loaded material was assessed by including ^{125}I-[Tyr^{116}]PTHrP(107-115) (200,000 c.p.m. or 140 fmol) as a tracer together with the cold peptide during peptide loading, as described elsewhere [8]. The radioactivity released into the incubation medium was sequentially monitored for several hours by counting in a γ-spectrometer.

2.3. Preparation of Si-HA scaffolds with covalently bound osteostatin

In order to prepare the scaffold surface to covalently bind osteostatin the Si-HA scaffolds prepared as mentioned above (with final dimensions 7 mm in diameter and 5 mm high) were organically functionalized employing (3-aminopropyl)triethoxysilane (APTES) (ABCR GmbH, Germany). Prior to this the scaffolds were dried at 90 °C under vacuum for 2 h. Then the scaffolds were refluxed in toluene with APTES under magnetic stirring overnight, followed by washing with ether and ethanol to remove the unreacted APTES and toluene. The organic (NH_2–) functionalization was confirmed through thermogravimetry and CHN elemental analysis. These scaffolds are denoted Si-HA(C) in the text.

The covalent grafting of osteostatin was performed through the formation of an amide bond between the hydroxyl groups of its C-terminal Trp and the amino groups on the scaffold surface. Trp was previously activated using [1-ethyl-3-(3-dimethylaminopropyl) carbodiimide] (EDC), which is usually employed as a carboxyl activating agent for the coupling of primary amines to yield amide bonds (Scheme 1) [12,13].

An aqueous solution buffered at pH 4.7 (acetate buffer) was employed to dissolve osteostatin (2 mg ml^{-1}) and then an excess of EDC was added and stirred at room temperature for 20 min (solution A). Separately, Si-HA(C) scaffolds were soaked in different vessels in an aqueous solution buffered at pH 8 (phosphate buffer) and 50 μl of solution A were then added to each scaffold vessel and stirred using an orbital shaker at room temperature for 12 h. Afterwards the scaffolds were washed several times with the same buffered solution to remove the non-attached osteostatin. For comparative purposes the same procedure was carried out without the use of EDC for osteostatin grafting.

2.4. Osteostatin grafting assessment

The grafting of osteostatin onto the surface of Si-HA(C) scaffolds was confirmed by Fourier transformed infrared (FTIR) spectroscopy (Thermo Nicolet Nexus spectrometer equipped with a Goldengate attenuated total reflectance device). Additionally, the amount of peptide grafted was quantified by measuring the peptide content in the washing solutions using reversed phase high performance liquid chromatography (RP-HPLC) in a Waters Alliance automatic analysis system (Waters, Mildford, MA) comprising a Model 2695 separations module and a Model 2996 photodiode array detector with a 250 × 4.6 mm and 5 μm C18 column (Mediterranea Sea18,

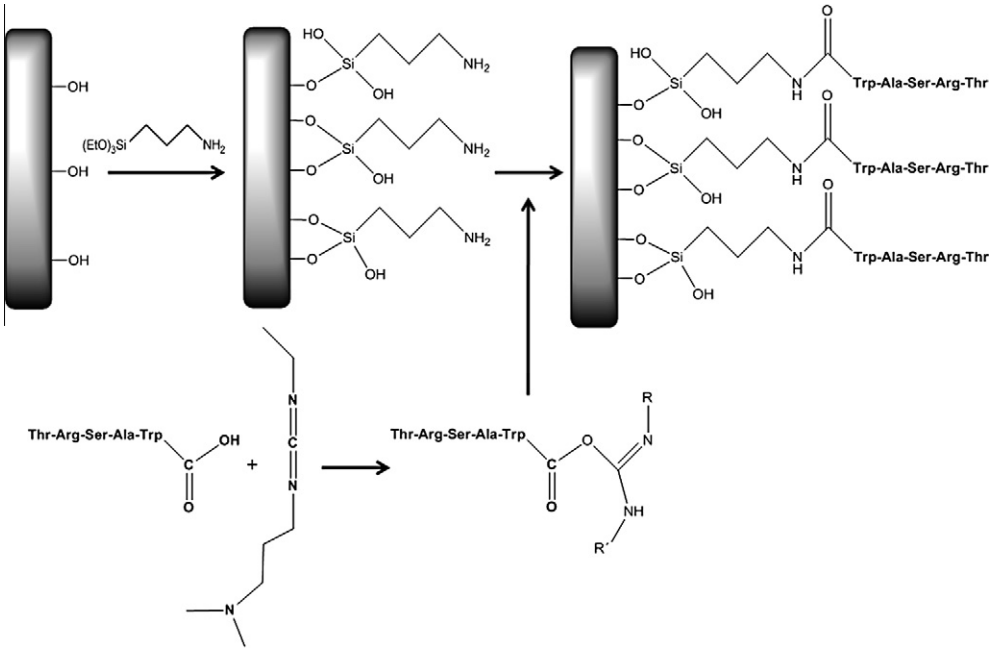

Scheme 1. Activation of PTHrP(107-111) and its subsequent coupling to primary amino groups on the Si-HA(C) scaffold surface.

Teknokroma, Barcelona, Spain). The mobile phase was composed of acetonitrile (HPLC grade, Sigma–Aldrich, St Louis, MO) with 1% trifluoroacetic acid (TFA) (Sigma–Aldrich) and water (HPLC grade, Sigma-Aldrich) with 1% TFA and a gradient of 0–50% acetonitrile for 25 min at a flow rate of 1 ml min^{-1}. Under these conditions the retention time of osteostatin was 12.4 min. Detection was performed by UV at 278 nm and chromatograms were recorded using Empower software. Several osteostatin solutions of varying concentrations (between 12.5 μg/l and 1 mg/ml) in 0.9% NaCl buffered at pH 7.4 were used as standards. The calibrated plot showed a correlation coefficient >0.999.

The scaffolds were sterilized before exposure to cell cultures by soaking them in ethanol (70%) and overnight exposition to UV radiation in a laminar flux cabin.

2.5. Cell cultures

To determine the osteogenic capacity of these peptide-modified scaffolds cell culture experiments were performed using the mouse osteoblastic cell line MC3T3-E1 [8]. The scaffolds tested (2.5 × 4 mm) were placed in each well of 6-well plates before cell seeding. Then MC3T3-E1 cells were plated at a density of 10,000 cells cm^{-2} in 2 ml of α-minimum essential medium (MEM) containing 10% fetal bovine serum (FBS), 50 μg ml^{-1} ascorbic acid, 10 mM β-glycerol 2-phosphate and 1% penicillin–streptomycin at 37 °C in 5% CO_2, and incubated for different times. Some wells contained no scaffolds as controls. In some experiments neutralizing rabbit polyclonal antiserum C7 against the N-terminus of osteostatin [14,15] at 1:100-dilution, and PTHrP(107-111) or [Cys^{101}-Gly^{102}-Gly^{103}-Ser^{104}-Gly^{105}-Gly^{106}]PTHrP(107-111) [CGGSGG-PTHrP (107-111)], each at 100 nM, were added to the culture medium for the time indicated below. The medium was replaced every other day.

In order to examine osteostatin immobilization and release from Si-HA scaffolds mouse pluripotent mesenchymal C3H10T1/2 cells, which can be committed to the osteoblast lineage in an osteogenic medium [16], were also used. These cells were maintained in Eagle's basal medium with 10% FBS and 1% penicillin–streptomycin in 5% CO_2 at 37 °C.

2.6. Cell growth

To evaluate cell proliferation a Cell-titer 96 Proliferation Kit (Promega, Madison, WI) was used following the manufacturer's instructions. Briefly, a solution containing 3-(4,5-dimethythizol-2-yl)-5-(3-carboxymethoxyphenyl)-2-(4-sulfophenyl)-2H-tetrazolium salt (MTS) and an electron coupling reagent (phenazine ethosulphate) (20 μl) was added to 100 μl of each cell-conditioned medium and incubated for 2 h. The absorbance at 490 nm was then measured. Cell viability was determined by collecting and pooling non-adherent and adherent cells (after gentle trypsinization), and staining with trypan blue as described [8]. The number of viable cells, which did not take up the stain, were counted in a haemocytometer.

2.7. Collagen production

Cell collagen production was evaluated using the Sircol™ collagen assay (Biocolor, Newtownabbey, UK) [8]. Following incubation

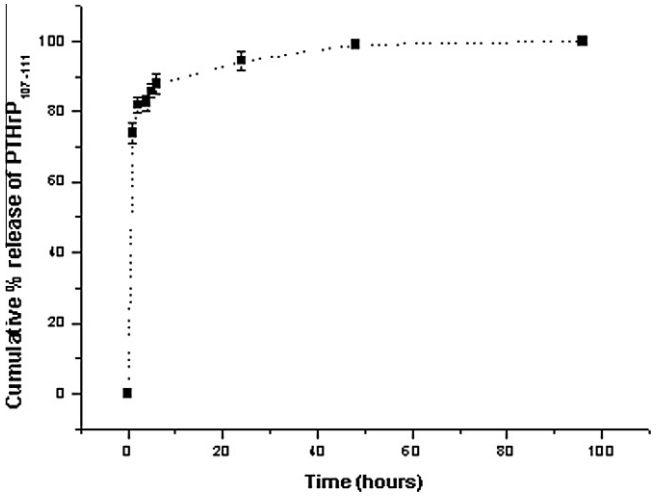

Fig. 1. PTHrP(107-111) release profile from Si-HA(A) scaffolds. Points tracing the curve are the means of five experiments.

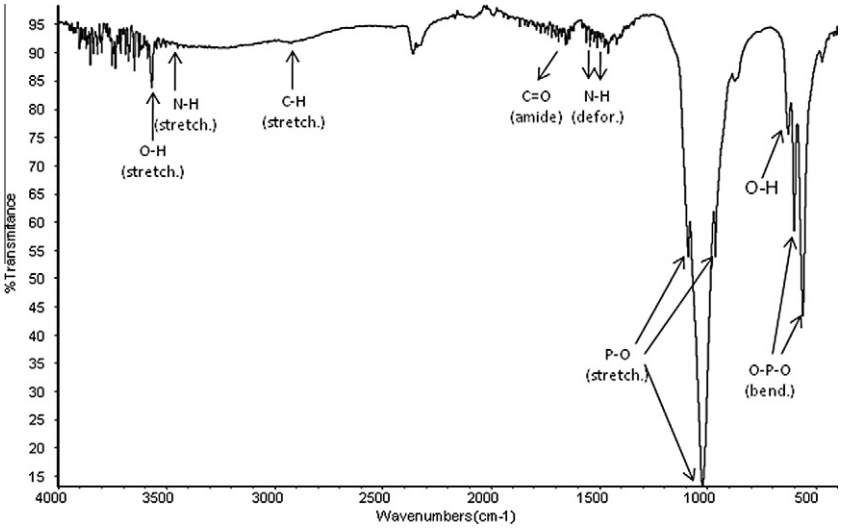

Fig. 2. FTIR spectra collected from a representative Si-HA(C) scaffold.

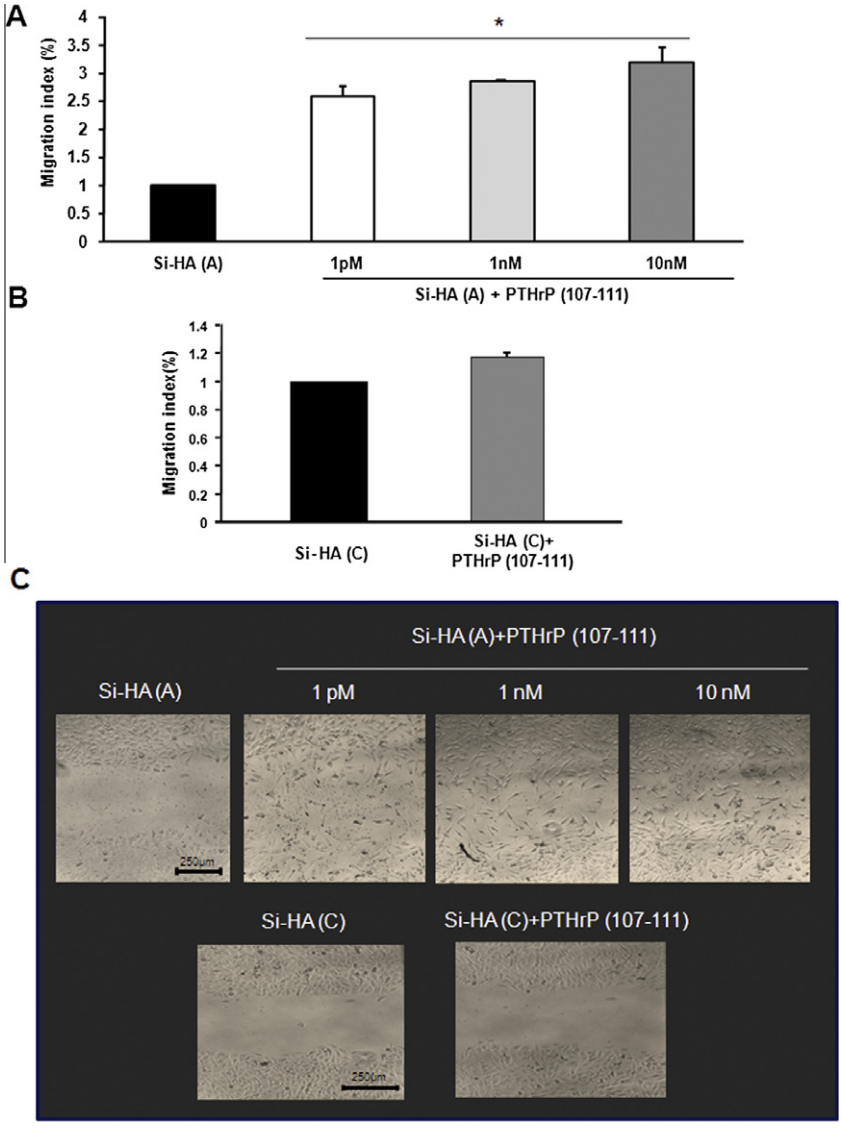

Fig. 3. Evaluation of different types of Si-HA scaffolds using the migration index in the scratch wound healing assay performed on C3H10T1/2 cell cultures, as described in the text. (A) Si-HA(A) scaffolds, precoated with different osteostatin concentrations or (B) Si-HA(C) scaffolds with covalently linked osteostatin were placed in Transwell chambers without physical contact with the cell monolayers on the culture plate surface. Results are means ± SEM of three measurements in triplicate. $^{\#}P < 0.05$ vs. non-coated Si-HA(A). Representative light microscopy images are also shown (magnification 50×).

with the tested materials for different times cells were sequentially collected by scraping into PBS, centrifuged at 1000*g* for 10 min, and then incubated in 0.5 M acetic acid. After centrifugation again as described the acid extract, which accounted for most of the initial cell pellet volume, was incubated with Sirius Red reagent for 30 min. The collagen-bound dye was quantified by measuring the absorbance at 540 nm, according to the manufacturer's instructions. Cell collagen was normalized to cell protein content, estimated as described above.

2.8. Mineralization assay

Matrix mineralization was measured by alizarin red staining after incubation of MC3T3-E1 cells with the tested materials for 12 days, as described elsewhere [2]. The stain was dissolved with 10% cetylpyridinum chloride in 10 mM sodium phosphate, pH 7, measuring the absorbance at 620 nm.

2.9. Scratch wound healing assay

C3H10 T1/2 cells were seeded at high density in order to create a monolayer (2×10^5 cells per well in a 12-well plate) in α-MEM supplemented with 10% FBS and 1% penicillin–streptomycin in CO_2 at 37 °C. The next day the cells were washed twice with PBS and then a scratch was made manually with a tip filter and subsequently washed twice with PBS [17]. Fresh medium with 1% FBS was then added, and a picture of the scratch in each well was taken with a DFC 420 C camera coupled to an DMI3000 inverted microscope (Leica Biosystems, Richmond, IL) with a 5× objective. To test the effect of released osteostatin from Si-HA(A) scaffolds they were presoaked in a peptide solution of varying concentrations (10 and 1 nM and 1 pM), as described above. Each Si-HA(A) or Si-HA(C) scaffold was then placed in a cell culture insert (Millipore, Billerica, MA) filled with 250 μl of culture medium. Scratch wound healing was evaluated at 24 h by taking images which were analyzed with Cellprofiler software (www.cellprofiler.org), as described [18]. The migration index was calculated by measuring the area covered by cells and comparing it with the initial area covered (time 0) for each well.

2.10. Statistical analysis

Results are expressed as means ± SEM. Statistical evaluation was carried out with non-parametric analysis of variance (Kruskal–Wallis test) and a post-hoc (Dunn's) test or Mann–Whitney test when appropriate. A value of $P < 0.05$ was considered significant.

3. Results and discussion

Firstly, the capacity of osteostatin-loaded Si-HA(A) scaffolds to release this peptide was assessed, using a previously described protocol [8]. At physiological pH electrostatic interaction is likely to be responsible for osteostatin coating this material. Consistent with the results obtained using another non-functionalized ceramic matrix [8], it was found that retention of osteostatin by Si-HA(A) scaffolds was (mean) 66% after 24 h loading; equivalent to 0.8 μg osteostatin g Si-HA(A)$^{-1}$. These scaffolds released (means) 74%, 93% and 100% of the loaded peptide to the surrounding medium after 1, 24 and 96 h, respectively. Peptide release is faster within the first 24 h, reaching a stationary phase later on (Fig. 1).

Secondly, cylindrical scaffolds of Si-HA(C) were evaluated. Successful grafting of amine groups onto these scaffolds was confirmed through CHN elemental analysis. Thus the percentage values of C (0.43%), H (0.23%) and N (0.18%) confirmed the presence of alkyl amino groups grafted onto the surface of the scaffolds. These low percentages revealed a low degree of functionalization, which could be accounted for by the low Si content, ~1%, of the scaffold [7]. The same trend was observed by thermogravimetry, showing a weight loss of ~1.2% after heating at between 200 and 300 °C, indicating 1.2% organic functionalization. Although this low value would prevent high percentage attachment of osteostatin, it is well known that even small amounts of active peptides grafted onto the surface of biomaterials can elicit dramatic biological effects. As an example, in the case of RGD peptides a surface density of only 1 fmol cm^{-2} effectively promotes cell adhesion to an otherwise non-adherent surface [19].

FTIR spectra collected from Si-HA(C) (Fig. 2) showed the characteristic absorption bands of carbonated HA [20]. Intense bands were also observed at approximately 1096, 1027 and 966 cm^{-1}

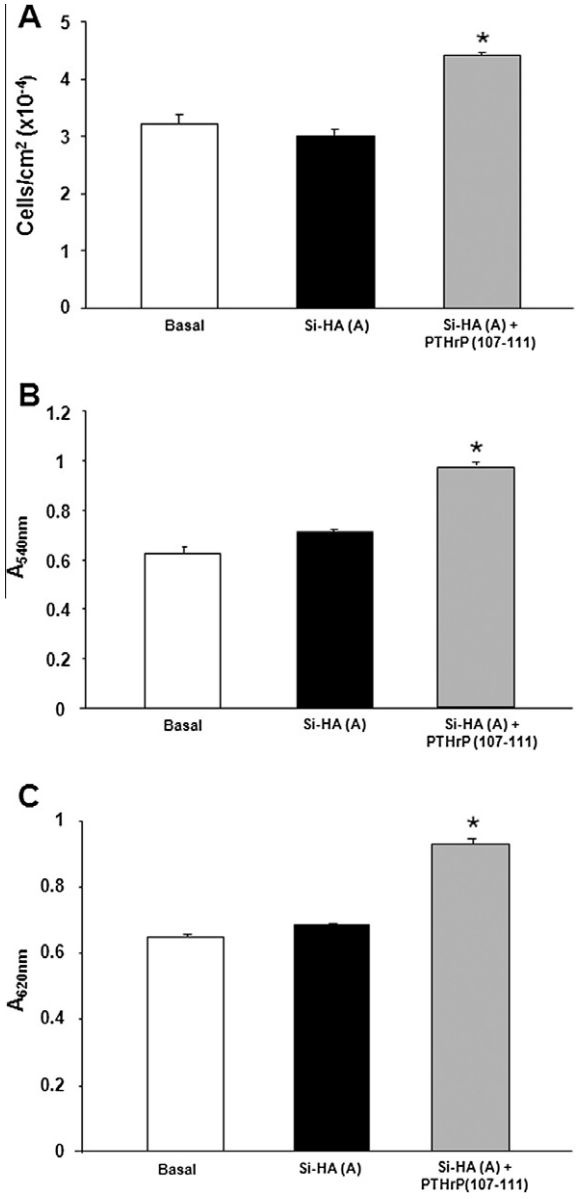

Fig. 4. (A) MC3T3-E1 cell viability assessed by trypan blue exclusion and (B) cell growth measured by CellTiter 96® AQueous assay as described in materials and methods in the presence or absence (basal) of Si-HA(A), loaded or not with 100 nM PTHrP(107-111) after 2 days culture. (C) Matrix mineralization (measured by Alizarin red staining) in these cells, in the presence or absence of the Si-HA(A) scaffolds, was assessed on day 12 of culture. Results are means ± SEM of four measurements in triplicate. $^{\#}P < 0.05$ vs. basal and non-coated Si-HA(A).

that correspond to P–O stretching vibration modes. The O–P–O bending mode was confirmed by the presence of bands at approximately 603 and 562 cm^{-1}. Additionally, the presence of the doublet at approximately 1459 and 1419 cm^{-1} confirmed the presence of CO_3^{2-}. The band at approximately 3568 cm^{-1}, assigned to O–H stretching, together with the band at approximately 633 cm^{-1}, due to the O–H vibrational mode, confirmed the presence of hydroxyl groups on Si-HA. The functionalization of Si-HA(C) with $-NH_2$ groups, even if it was at a low degree as mentioned above, was confirmed by the presence of the stretching vibration bands at approximately 3488 cm^{-1}, together with the presence of N–H deformation bands at approximately 1530–1570 cm^{-1}, which are typical of N–H bonds. The presence of more intense bands at approximately 2938 and 2880 cm^{-1} can be attributed to C–H stretching vibrations from the aminopropyl silane groups. The grafting of osteostatin onto this type of scaffold was confirmed by the presence of a weak vibration band at approximately 1647 cm^{-1}, which can be attributed to the newly formed amide bond between functionalized alkoxisilanes on the scaffold surface and the C-terminal Trp in osteostatin. It should be pointed out that the observed C=O stretching band might also be produced by amide bonds in the peptide itself. However, this is unlikely based on the fact that during the synthetic procedure, and immediately after the functionalization process, the scaffold pieces were vigorously washed several times with buffer solution. In this way all peptide moieties that were not strongly grafted to the scaffold surface would have been washed away. Thus if peptide molecules are detected (through amide vibration bands) they must be covalently attached to the Si-HA(C) scaffolds. The amount of osteostatin grafted onto the surface of the latter scaffolds was determined by its remaining concentration in the stock solution after the loading process, as determined by RP-HPLC. The observed retention time of the pentapeptide was ~12.4 min, and it was detected by UV absorption at ~280 nm. Based on this procedure, osteostatin grafting on amino-modified Si-HA(C) scaffolds represented on average 20 μg peptide per 190 mg scaffold used for each bioassay described below.

Osteostatin immobilization was confirmed by chemical analysis and by testing the efficiency of both types of osteostatin-loaded Si-HA scaffolds (placed in Transwell chambers) to heal a scratch wound in a mesenchymal C3H10T1/2 cell layer. We found that exposure of wounded monolayers of these cells to Si-HA(A) scaffolds releasing osteostatin in the picomolar to nanomolar range dramatically accelerated wound healing at 24 h (Fig. 3A and B). This is an interesting finding which strongly supports the putative usefulness of osteostatin-coated Si-HA scaffolds as implants to promote bone healing. On the other hand, osteostatin-containing Si-HA(C) scaffolds, similarly to non-coated Si-HA(A) scaffolds, were inefficient in this regard in this assay (Fig. 3A and B). These data indicate the stability of the amide bond used to bind osteostatin to the Si-HA(C) scaffold surface in the presence of cell-conditioned medium. In this regard, the short osteostatin sequence does not appear to be sensitive to any known protease action [21]. In fact, zinc metallopeptideses such as PHEX (phosphate-regulating gene with homologies to endopeptidases on the X chromosome) protein and neprylysin, which are abundant in osteoblasts, can digest the native human peptide PTHrP(107-139) by targeting sites distal to the osteostatin sequence [22,23].

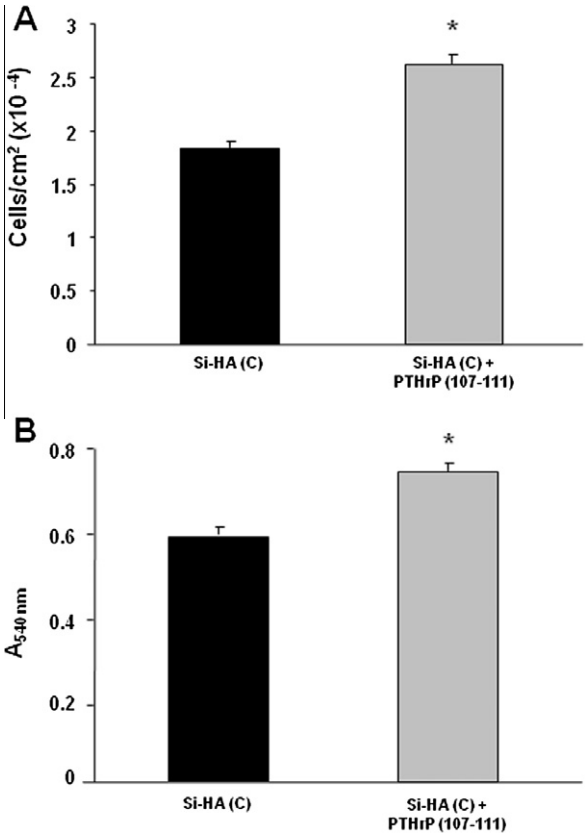

Fig. 5. MC3T3-E1 (A) cell viability and (B) cell growth determined as in the legend to Fig. 4, in the presence or absence (basal) of Si-HA(C), loaded or not with PTHrP(107-111), after 2 days. Results are means ± SEM of four measurements in triplicate. $^{\#}P < 0.05$ vs. Si-HA(C).

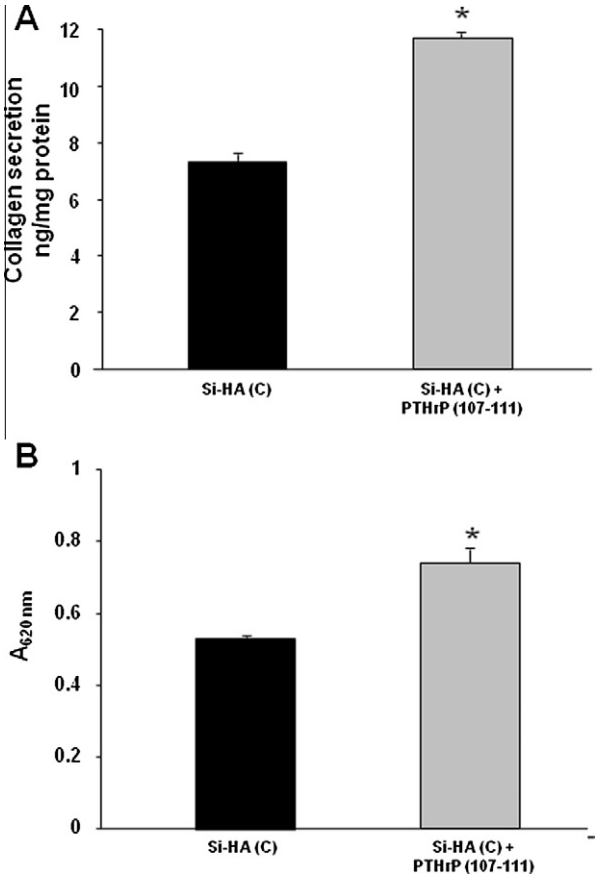

Fig. 6. (A) Collagen production and (B) matrix mineralization in MC3T3-E1 cells, in the presence or absence of Si-HA(C) scaffolds, on days 2 and 12, respectively. The results are means ± SEM of four measurements in triplicate. $^{\#}P < 0.05$ vs. non-coated Si-HA(C).

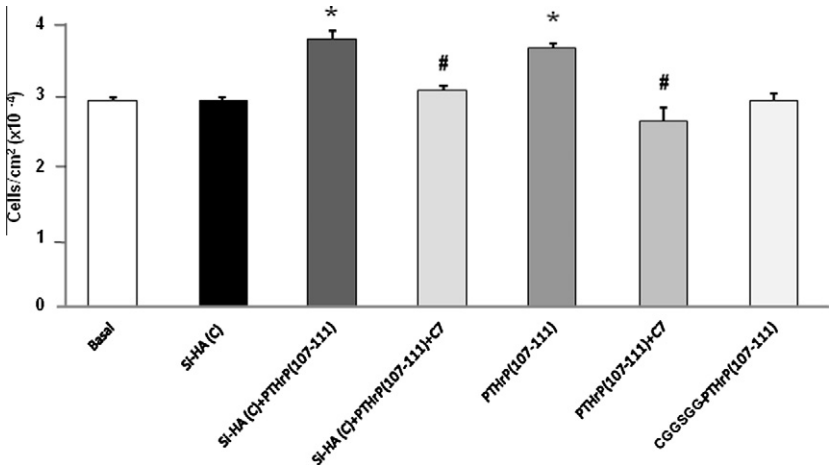

Fig. 7. MC3T3-E1 cell viability (determined by trypan blue exclusion) in the presence or absence (basal) of Si-HA(C), loaded or not with PTHrP(107-111) or CGGSGG–PTHrP(107-111) (each at 100 nM) on day 2. When present, neutralizing osteostatin antiserum C7 was used at 1:100 dilution. The results are means ± SEM of three measurements in triplicate. $^{*}P < 0.05$ vs. Si-HA(C) or the basal value; $^{\#}P < 0.05$ vs. the corresponding value without antiserum C7.

We next assessed in a comparative manner the bioactivity conferred by osteostatin to both types of Si-HA (A and C) scaffolds using osteoblastic cell cultures. We found that exposure to Si-HA(A) loaded with osteostatin by adsorption, in contrast to the unloaded scaffold, increased MC3T3-E1 cell growth on day 2 of culture (Fig. 4A and B). As shown by the osteostatin release kinetics, its concentration in the cell culture medium at this time was about 100 nM, at which it was shown to maximally stimulate osteoblastic cell growth in this and other osteoblastic cell types [8,24].

Osteostatin covalently bound to Si-HA(C) scaffolds was also shown to have a similar stimulatory effect on MC3T3-E1 cell growth within 2 days of exposure to this material (Fig. 5). In addition, this type of scaffold containing osteostatin significantly stimulated collagen production in the same time period in these cells (Fig. 6A). Similar bioactivities were observed on omitting the use of EDC for osteostatin grafting to this type of scaffold (not shown), suggesting that using EDC did not significantly increase the amidation reaction yield on the Si-HA(C) scaffold surface. Finally, none of the tested Si-HA scaffolds were found to affect cell growth of or matrix mineralization by MC3T3-E1 cells, indicating that osteostatin confers this bioactivity on the scaffolds (Figs. 3–6).

Interestingly, both types of scaffolds, Si-HA(A) and Si-HA(C), containing osteostatin promoted matrix mineralization by MC3T3-E1 cells on day 12 of culture (Figs. 4C and 6B). These data thus demonstrate that osteostatin, either released or covalently bound by its C-terminus to Si-HA scaffolds, can be similarly efficient in inducing osteoblastic function. This finding is interesting and adds credence to the hypothesis that the N-terminal region of osteostatin, particularly its first amino acid (Thr), might be essential for its bioactivity in bone cells [25]. In further support of this notion, the presence of a neutralizing anti-osteostatin antiserum against the N-terminus abolished the osteostatin effect on osteoblastic cell growth, as observed with the synthetic peptide and when bound to Si-HA(C) (Fig. 7). Moreover, a peptide comprising osteostatin with an extended amino acid sequence at its N-terminus was inefficient in this respect (Fig. 7). Of note, the native PTHrP(107-139) fragment has been shown to exert several activities mimicked by osteostatin in various osteoblastic cell preparations [14,15,24,26]. Indeed, analysis of PTHrP(107-139) in solution by nuclear magnetic resonance spectroscopy indicates that the osteostatin region, in contrast to the rest of the sequence, forms an extended finger-like structure which is likely to interact with a specific receptor on target cells [27].

The present findings also show that exposure to decreasing amounts of osteostatin remaining on Si-HA(A) scaffolds or to continuous low concentrations of this peptide on the surface of Si-HA(C) scaffolds, likely in the nanomolar or lower range based on the scaffold size, can similarly induce matrix mineralization by osteoblastic cells. In this regard, previous studies have reported the ability of osteostatin to affect cell growth and function at nanomolar and even lower concentrations using various bone cell preparations [8,14,24,26,28].

These results indicate that local delivery of osteostatin is not essential for this peptide to induce osteogenic features, an interesting observation within the frame of the potential clinical usage of Si-HA scaffolds. This notion is consistent with our previous observations suggesting that the improved performance in vitro and in vivo of non-degradable C8-SBA-15 bioceramics with an osteostatin coating might be accounted for by the increased local concentration of this peptide in the osteoblastic cell microenvironment [8,10].

4. Conclusions

The exposure of MC3T3-E1 cell monolayers to Si-HA scaffolds coated with osteostatin, both deliverable and immobilized, stimulated cell growth and matrix mineralization. These in vitro data demonstrate that Si-HA as scaffolds coated with osteostatin display osteoblastic activities which make them likely to promote bone formation in vivo. It remains to be examined whether osteostatin immobilization by covalent bonding onto these scaffolds might represent an advantage to accelerate skeletal repair in vivo.

Acknowledgements

We are indebted to F. Roncal Ph.D. (Proteomics Unit, Centro Nacional de Biotecnología, Consejo Superior de Investigaciones Científicas, Madrid) for CGGSGG–PTHrP(107-111) synthesis. This research was supported by Grants from the Spanish Ministerio de Ciencia e Innovación (MAT2008-00736, SAF2005-05254, PI080922 and RETICEF RD06/0013/1002), the Fundación de Investigación Médica Mutua Madrileña, and the Comunidad Autónoma de Madrid (S2009 MAT-1472).

Appendix A. Figures with essential colour discrimination

Certain figure in this article, particularly Figure 3, is difficult to interpret in black and white. The full colour images can be found in the on-line version, at doi:10.1016/j.actbio.2011.06.004.

References

[1] Vallet-Regí M, Arcos D. Biological apatites in bone and teeth. In: O'Brien P, Kroto H, Craighead H, editors. Biomimetic nanoceramics in clinical use. From materials to applications. Cambridge: RSC Publishing; 2008. p. 1–24.

[2] Yaszemski MJ, Payne RG, Hayes WC, Langer R, Mikos AG. Evolution of bone transplantation: molecular, cellular and tissue strategies to engineer human bone. Biomaterials 1996;17:175–85.

[3] We G, Ma PX. Nanostructured biomaterials for regeneration. Adv Funct Mater 2008;18:3568–82.

[4] Hutmacher DW. Scaffolds in tissue engineering bone and cartilage. Biomaterials 2000;21:2529–43.

[5] Frieb W, Werner J. Biomedical applications. In: Schüth F, Kienneth S, Sing W, Kamps W, editors. Handbook of porous solids. Weinheim: Wiley-VCH; 2000. p. 2923–70.

[6] Leong KF, Cheah CM, Chua CK. Solid freeform fabrication of three-dimensional scaffolds for engineering replacement tissues and organs. Biomaterials 2003;24:2363–78.

[7] Balas F, Pérez-Pariente J, Vallet-Regí M. In vitro bioactivity of silicon-substituted hydroxyapatites. J Biomed Mater Res 2003;66A:364–75.

[8] Lozano D, Manzano M, Doadrio JC, Salinas AJ, Vallet-Regí M, Gómez-Barrena E, et al. Osteostatin-loaded bioceramics stimulate osteoblastic growth and differentiation. Acta Biomater 2010;6:797–803.

[9] Kohane DS, Langer R. Biocompatibility and drug delivery systems. Chem Sci 2010;1:441–6.

[10] Trejo CG, Lozano D, Manzano M, Doadrio JC, Salinas AJ, Dapía S, et al. The osteoinductive properties of mesoporous silicate coated with osteostatin in a rabbit femur cavity defect model. Biomaterials 2010;31:8564–73.

[11] Arcos D, Rodríguez-Carvajal J, Vallet-Regí M. Silicon incorporation in hydroxylapatite obtained by controlled crystallization. Chem Mater 2004;16:2300–8.

[12] Barrera DA, Zylstra E, Lansbury Jr PT, Langer R. Synthesis and RGD peptide modification of a new biodegradable copolymer: poly(lactic acid-co-lysine). J Am Chem Soc 1993;115:11010–1.

[13] Cook AD, Hrkach JS, Ga NN, Johnson IM, Pajvani UB, Cannizzaro SM, et al. Characterization and development of RGD-peptide-modified poly(lactic acid-co-lysine) as an interactive, resorbable biomaterial. J Biomed Mat Res 1997;35:513–23.

[14] Valín A, García-Ocaña A, De Miguel F, Sarasa JL, Esbrit P. Antiproliferative effect of the C-terminal fragments of parathyroid hormone-related protein, PTHrP-(107–111) and (107–139), on osteoblastic osteosarcoma cells. J Cell Physiol 1997;170:209–15.

[15] Lozano D, Fernández-de-Castro L, Portal-Núñez S, López-Herradón A, Dapía S, Gómez-Barrena E, et al. The C-terminal fragment of parathyroid hormone-related peptide promotes bone formation in diabetic mice with low turnover osteopaenia. Br J Pharmacol 2011;162:1424–38.

[16] Chan GK, Miao D, Deckelbaum R, Bolivar I, Karaplis A, Goltzman D. Parathyroid hormone-related peptide interacts with bone morphogenetic protein 2 to increase osteoblastogenesis and decrease adipogenesis in pluripotent C3H10T 1/2 mesenchymal cells. Endocrinology 2003;144:5511–20.

[17] Menon MB, Ronkina N, Schwermann J, Kotlyarov A, Gaestel M. Fluorescence-based quantitative scratch wound healing assay demonstrating the role of MAPKAPK-2/3 in fibroblast migration. Cell Motil Cytoskel 2009;66:1041–7.

[18] Lamprecht MR, Sabatini DM, Carpenter AE. CellProfiler™: free, versatile software for automated biological image analysis. BioTechniques 2007;42:71–5.

[19] Massia SP, Hubbell JA. An RGD spacing of 440 nm is sufficient for integrin alpha V beta 3-mediated fibroblast spreading and 140 nm for focal contact and stress fiber formation. J Cell Biol 1991;114:1089–100.

[20] Fowler BO. Infrared studies of apatites. II. Preparation of normal and isotopically substituted calcium, strontium, and barium hydroxyapatites and spectra–structure–composition correlations. Inorg Chem 1974;13:207–14.

[21] Yang KH, dePapp AE, Soifer NE, Dreyer BE, Wu TL, Porter SE, et al. Parathyroid hormone-related protein: evidence for isoform- and tissue-specific posttranslational processing. Biochemistry 1994;33:7460–9.

[22] Ruchon AF, Marcinkiewicz M, Ellefsen K, Basak A, Aubin J, Crine P, et al. Cellular localization of neprilysin in mouse bone tissue and putative role in hydrolysis of osteogenic peptides. J Bone Miner Res 2000;15:1266–74.

[23] Boileau G, Tenenhouse HS, Desgroseillers L, Crine P. Characterization of PHEX endopeptidase catalytic activity: identification of parathyroid-hormone-related peptide 107–139 as a substrate and osteocalcin, PPi and phosphate as inhibitors. Biochem J 2001;355:707–13.

[24] Cornish J, Callon KE, Lin C, Xiao C, Moseley JM, Reid IR. Stimulation of osteoblast proliferation by C-terminal fragments of parathyroid hormone-related protein. J Bone Miner Res 1999;14:915–22.

[25] Fenton AJ, Kemp BE, Hammonds RG, Mitchelhill K, Moseley JM, Martin TJ, et al. A potent inhibitor of osteoclastic bone resorption within a highly conserved pentapeptide region of PTHrP (107–111). Endocrinology 1991;129:3424–6.

[26] Valín A, Guillén C, Esbrit P. C-terminal parathyroid hormone-related protein (PTHrP) (107–139) stimulates intracellular $Ca2^{+}$ through a receptor different from the type 1 PTH/PTHrP receptor in osteoblastic osteosarcoma UMR 106 cells. Endocrinology 2001;142:2752–9.

[27] Cuthbertson RM, Kemp BE, Barden JA. Structure study of osteostatin PTHrP[Thr107](107–139). Biochim Biophys Acta 1999;1432:64–72.

[28] Zheng MH, McCaughan HB, Papadimitriou JM, Nicholson GC, Wood DJ. Tartrate resistant acid phosphatase activity in rat cultured osteoclasts is inhibited by a carboxyl terminal peptide (osteostatin) from parathyroid hormone-related protein. J Cell Biochem 1994;54:145–53.